Hazard zoning for volcanic ballistic impacts at El Chichón Volcano (Mexico)

Miguel A. Alatorre-Ibargüengoitia, Horacio Morales-Iglesias, Silvia G. Ramos-Hernández, Juan Jon-Selvas & Julio M. Jiménez-Aguilar

ONLINE FIRST

Springer

Springer

CrossMark

ORIGINAL PAPER

Hazard zoning for volcanic ballistic impacts at El Chichón Volcano (Mexico)

Miguel A. Alatorre-Ibargüengoitia[1] · Horacio Morales-Iglesias[1] ·
Silvia G. Ramos-Hernández[1] · Juan Jon-Selvas[1] ·
Julio M. Jiménez-Aguilar[1]

Abstract   The 1982 eruption of El Chichón Volcano in southeastern Mexico had a strong social, economic, and environmental impact. The eruption gave rise to the most disastrous volcanic events in Mexico, killing around 2000 inhabitants, displacing thousands, and resulting in severe economic losses. Despite some villages were relocated after this eruption, many people still live and work in the vicinities of the volcano and might be affected in the case of a new eruption. For this reason, it is important to identify the exposed zones. The published hazard map of El Chichón Volcano covers pyroclastic flows and surges, lahars, and ashfall, but not ballistic projectiles, which would represent an important threat in the case of an eruption. In fact, the fatalities reported in the first stage of the 1982 eruption were caused by ballistic projectiles and ashfall that induced roof collapse. In this study, the hazard zones for volcanic ballistic projectiles at El Chichón Volcano are delimited through a general methodology that has been applied to other volcanoes such as Popocatépetl (Alatorre-Ibarguengoitia et al. in Bull Volcanol 74:2155–2169, 2012. doi:10.1007/s00445-012-0657-2) and Colima (Alatorre-Ibarguengoitia et al. in Geol Soc Am Spec Paper 402:26–39, 2006). The maximum launching kinetic energy of projectiles identified in the field corresponding to past eruptions is reconstructed by using a ballistic model. These energies are then used to parameterize different explosion scenarios that can occur in the future. The maximum ranges expected for the projectiles in the different explosive scenarios defined for El Chichón Volcano are presented in a ballistic hazard map which complements the published hazard map. The responsible authorities may use this map to be able to mark off the restricted zones during volcanic crises.

Keywords   Volcanic hazard · Volcanic eruption · El Chichón Volcano · Hazard map · Ballistic projectiles · Pyroclasts ejection

✉ Miguel A. Alatorre-Ibargüengoitia
    miguel.alatorre@unicach.mx; alatorre.miguel@gmail.com

[1]   Centro de Investigación en Gestión de Riesgos y Cambio Climático, Universidad de Ciencias y Artes de Chiapas, Libramiento Norte Pte. #1150 Col. Lajas Maciel, 29039 Tuxtla Gutiérrez, Mexico

Springer

1 Introduction

El Chichón Volcano (17.36°N, 93.23°W), located in the State of Chiapas, southeastern Mexico (Fig. 1), is the youngest member of the Chiapanecan Volcanic Arc (Mora et al. 2012) and has a violent eruptive record in the Holocene with at least 12 major eruptions in the past 8000 years (Tilling et al. 1984; Espíndola et al. 2000; Layer et al. 2009; Scola-macchia and Capra 2015). Its last eruption was in 1982 and gave rise to the most disastrous volcanic events in Mexico, killing around 2000 inhabitants, displacing thousands, and resulting in severe economic losses (De la Cruz-Reyna and Martin Del Pozzo 2009). The disaster had several causes, including the inaccessibility of the area and lack of a monitoring system and volcano hazard map (Macías et al. 2008). After this eruption, abundant information has been collected about its Holocene eruptive registry (Tilling et al. 1984; Duffield et al. 1984; Rose et al. 1984; Espíndola et al. 2000; Macías et al. 2003), its
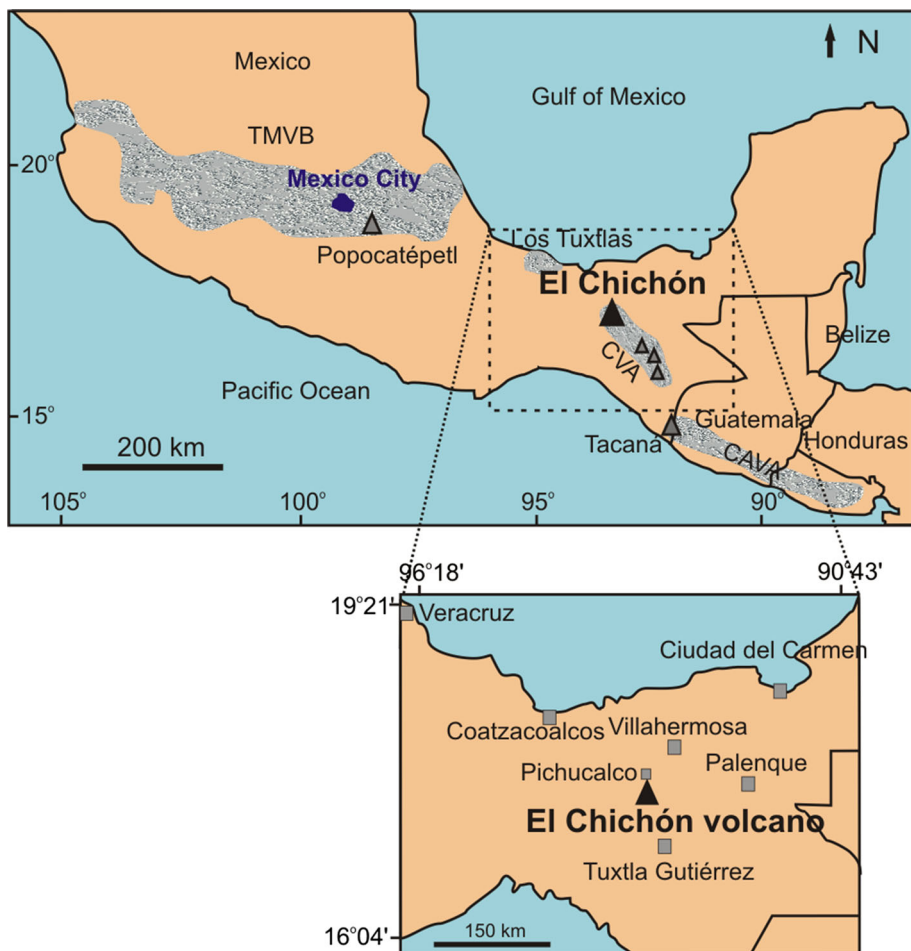
Fig. 1 Location of El Chichón Volcano in southern Mexico. *TMVB* Trans-Mexican Volcanic Belt, *CVA* Chiapanecan Volcanic Arc, *CAVA* Central American Volcanic Arc

geothermal activity (Taran et al. 1998; Tassi et al. 2003; Capaccioni et al. 2004; Rouwet et al. 2004; Armienta et al. 2000, 2014), and geophysical data obtained in real time from a seismic network installed in 2004 operated by Centro de Investigación en Gestión de Riesgos y Cambio Climático, Universidad de Ciencias y Artes de Chiapas. With the available information, Macías et al. (2008) presented a hazard map of El Chichón Volcano which shows the areas that might be affected in future eruptions by pyroclastic flows and surges, lahars, and fall. However, this map does not include volcanic ballistic projectiles (VBP) which produced several casualties and damage during the 1982 eruption, in particular during the first stage on 28 March (De la Cruz-Reyna and Martin Del Pozzo 2009). These projectiles represent also a significant threat for future eruptions, and therefore, it is important to estimate the zones that might be affected by these products. Here, we present the hazard map for ballistic impacts at El Chichón Volcano which complements the hazard map published by Macías et al. (2008).

2 Eruptive activity and ballistic projectiles of El Chichón Volcano

Pre-holocene eruptive activity of El Chichón Volcano occurred in several volcanic structures, mostly domes and ancient craters that are no longer active (Scolamacchia and Capra 2015). The Holocene stratigraphic record of this volcano consists of at least 12 eruption deposits with most of the repose intervals lasting between 100 to 600 years (Macías et al. 2008). These eruptions occurred in 1982 AD, and around 550, 900, 1250, 1500, 1600, 1900, 2000, 2500, 3100, 3700, and 7700 years BP (Rose et al. 1984; Tilling et al. 1984; Espíndola et al. 2000). The 1982 event erupted an estimate of 1.1 km³ of magma of dense rock equivalent (Carey and Sigurdsson 1986) and formed three sustained Plinian columns higher than 27 km with associated pyroclastic density currents that devastated an area of about 10 km around the volcano and covered southeastern Mexico with ash fall (De la Cruz-Reyna and Martin Del Pozzo 2009). According to Macías et al. (2003), the eruptive column of the 550 BP eruption reached an altitude of around 31 km and covers a larger area. It is believed that the 550-, 1250-, and 3700-year BP eruptions were larger or similar in magnitude to the 1982 eruption. In contrast with this last eruption, nowadays the crater is open and occupied by a lake, apparently as it was before during the 550-, 900-, 2000-, and 2500-year BP eruptions (Macías et al. 2008).

In order to recognize the ballistic projectiles with maximum range ejected during the eruptions of El Chichón Volcano, we performed an extensive survey of the whole area in three field campaigns in 2013 and 2014. We noticed that there are no impact craters anymore and it is complicated to identify impact sags due to the emplacement of subsequent volcanic products, heavy rains typical of tropical weather, and flourishing vegetation. In spite of these difficulties, we were able to identify 18 projectiles associated with impact sags indicating their ballistic emplacement (Fig. 2). We cannot exempt the chances that these projectiles were taken upward for some distance before they separated from the eruptive column and follow near parabolic paths (see 'Ballistic model'). Although abundant impact sags are reported in the moat area (Macías et al. 1997), i.e., the annular lowland between the new crater and the walls of the old Somma crater, our attention was put especially on the VBP found at farther distance from the vent due to their higher relevance for hazard assessment. Most of the projectiles are relatively dense and angular. GPS (Global Positioning System) was used in order to map out the location of each fragment. For each VBP, we measured three perpendicular axes and took the geometrical

average and we also weighed some of them in the field. Additionally, various VBP samples' densities were measured in the laboratory. Their average diameter ranges from 0.12 to 0.26 m, and their density from 1450 to 2549 kg/m^3 (Table 1). We found ballistic projectiles ejected in the 1982 eruption at distances up to 4.1 km from the crater and VBP ejected in the 550 BP eruption at a maximum distance of 5.2 km from the crater.
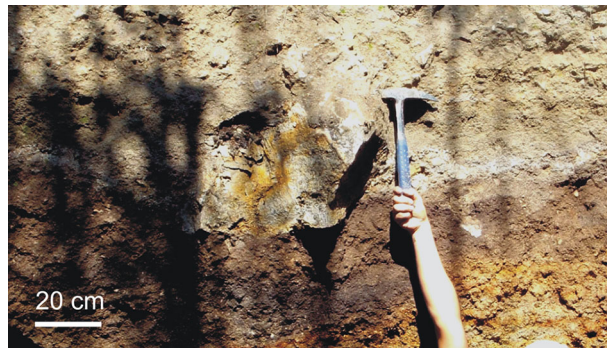
Fig. 2 Photograph of ballistic projectile B15 (Table 1) recognized in the field as ejected during the 1982 eruption of El Chichón Volcano. It is possible to identify a ballistic sag associated with the projectile

Table 1 Characteristics of the ballistic projectiles ejected during two different eruptions of El Chichón Volcano that were identified in the field in three campaigns

Projectile	Mean diameter (m)	Density (kg/m^3)	Distance (km)	Eruption
B1	0.15	2480	4.0	1982
B2	0.12	1714	4.1	1982
B3	0.12	2326	4.1	1982
B4	0.30	2480	2.4	1982
B5	0.22	2513	2.7	1982
B6	0.17	2310	3.9	1982
B7	0.16	2350	4.0	1982
B8	0.19	2208	4.1	1982
B9	0.18	2549	4.1	1982
B10	0.20	2380	2.8	1982
B11	0.16	1452	4.1	1982
B12	0.12	2106	4.2	1982
B13	0.22	2341	2.7	1982
B14	0.26	2542	2.5	1982
B15	0.22	2451	2.9	1982
B16	0.23	2203	2.9	1982
B17	**0.16**	**1589**	**5.2**	**550 BP**
B18	**0.16**	**1620**	**5.1**	**550 BP**

Bold text corresponds to the ballistic projectiles ejected during the 550 BP eruption

The mean diameter corresponds to the geometrical average of three perpendicular diameters measured for each projectile. This geometrical average represents the diameter of a sphere with the same volume. Density was measured in the laboratory using the Archimedean principle. The distance was calculated from the center of the crater formed after the 1982 eruption

3 Ballistic model

The initial velocities required to eject the VBP up to the distances where they were found in the field can be calculated using a ballistic model considering that during flight, these projectiles are subjected mainly to gravity and drag forces. The ballistic equation derived from Newton's second law can be expressed in a rectangular coordinate system as follows (Wilson 1972; Waitt et al. 1995; Alatorre-Ibargüengoitia and Delgado-Granados 2006):

$$\frac{dv_x}{dt} = -\frac{A\rho_a C_d(v_x - u_x)|\mathbf{v} - \mathbf{u}|}{2m} \tag{1a}$$

$$\frac{dv_z}{dt} = -\frac{A\rho_a C_d v_z|\mathbf{v} - \mathbf{u}|}{2m} - g \tag{1b}$$

where x and z represent the horizontal and vertical position coordinates, respectively, t is time, $\mathbf{v} = (v_x, v_z)$ represents the velocity vector of the projectile, A and m are the cross-sectional area and VBP mass, respectively, ρ_a is air density, C_d is the drag coefficient, $\mathbf{u} = (u_x, 0)$ represents the wind velocity vector (only considering horizontal wind velocity u_x), $|\mathbf{v} - \mathbf{u}| = \sqrt{(v_x - u_x)^2 + v_z^2}$, whereas g represents gravitational acceleration. For ellipsoidal VBP, the ratio $A/m = 3/(2\rho_b D)$, where D is the geometric mean of the three perpendicular axes and ρ_b is the projectile density. For the calculation of the trajectory of each projectile observed in the field, we used its corresponding density measured in the laboratory, whereas for general calculations that were not associated with a specific projectile, we used an average density of 2200 kg/m^3. Air density diminishes with altitude and can be expressed as a quadratic function fitting published altitude–density data (e.g., Waitt et al. 1995). We used C_d values corresponding to volcanic fragments measured in a subsonic wind tunnel (Alatorre-Ibargüengoitia and Delgado-Granados 2006). Along the trajectory, we use a fourth-order Runge–Kutta method so as to integrate numerically Eq. 1a and 1b following the scheme described by Wilson (1972). When the VBP vertical position (z) reaches a specified landing elevation (z_f), calculations are bring to an end.

Several visual observations of different eruptions and theoretical ballistic models reveal that the VBP are first taken upward and then pushed out into an expanding gas cloud that diminishes the drag force near the vent in a significant way (Fagents and Wilson 1993; Bower and Woods 1996; de' Michieli Vitturi et al. 2010; Konstantinou 2015; Taddeucci et al. 2015). If VBP were ejected into a stationary atmosphere, the drag force would increase dramatically, which in turn would result into extremely high initial velocity of these projectiles that would be required to achieve the observed distances (Fagents and Wilson 1993; Waitt et al. 1995; de' Michieli Vitturi et al. 2010; Swanson et al. 2010; Fitzgerald et al. 2014; Taddeucci et al. 2015).

So as to deal with this effect, we considered the method proposed by Fagents and Wilson (1993) and considered that all the pyroclasts accelerate coherently up to a certain radial distance from the vent R_o in a time t_o. At this point, the VBP are ejected with a velocity v_o into a gas that expands with velocity v_g, which decreases with distance from the vent R and time t according to the following expression:

$$v_g = v_o\left(\frac{R_o}{R}\right)^2 \exp(-t/\tau) \tag{2}$$

where the time constant τ is proposed to be related to the ratio of initial gas pressure (P_g) to atmospheric pressure (P_a) (Fagents and Wilson 1993):

$$\tau = \frac{P_g}{P_a} t_o \tag{3}$$

In a similar way, a drag coefficient region within an arbitrary distance from the vent was incorporated by Mastin (2001). In such approaches, the VBP are supposed to be ejected into an expanding gas that is moving with a certain velocity. More recently, Fitzgerald et al. (2014) considered a radius with an effective gas flow velocity that also decreases the drag force in the vicinities of the vent, and de' Michieli Vitturi et al. (2010) introduced a Lagrangian particle model that presents the ejection of volcanic clasts paired up with a multiphase model of the carrier flow. This model included the acceleration phase and also showed that the dynamics of the carrier flow determines the trajectories of even meter-sized pyroclasts. According to this model, a great deal of control is exerted on the ejection of individual VBP by the initial position of the particles and the near-vent geometry of the conduit, for which we require more sophisticated models (e.g., de' Michieli Vitturi et al. 2010) that are beyond the scope of this work. Furthermore, the model presented here cannot be used to investigate the general distribution of the VBP (e.g., Fitzgerald et al. 2014) since it does not consider the collisions of the fragments that may occur during the eruption (Vanderkluysen et al. 2012; Tsunematsu et al. 2014). Limitations considered, the simple ballistic model presented in this section, can be used to estimate the initial velocity of the VBP that reached the observed range in a particular eruption and subsequently to estimate the maximum distance that the VBP can travel at given ejection conditions.

4 Definition of explosion scenarios of El Chichón Volcano

The hazard zones that can be affected by VBP impact depend on the dynamics of the volcanic explosions that produces them. For this reason, it is indispensable to establish in a realistic and comprehensive manner diverse explosion scenarios which can produce and eject these projectiles in a particular volcano in accordance with its previous activity. Such explosion scenarios can be parameterized in terms of the maximum initial kinetic energy associated with individual ballistic projectiles (Alatorre-Ibargüengoitia et al. 2006, 2012). As mentioned above, the VBP are accelerated and ejected into an expanding gas cloud which significantly affects the trajectories of even meter-sized particles in the vicinity of the vent. It is the eruptive dynamics what determines the influence of the carrier flow on the VBP close to the vent, but this effect has not yet been fully understood (Taddeucci et al. 2015). According to the considered parameterization, the kinetic energy of individual VBP consists of the energy associated with their ejection velocity plus the added up energy which is transferred to the projectiles from the carrier. Consequently, the methodology proposed here is based on the assumption that all the eruptive processes that promote the ejection of the projectiles are gathered together into their corresponding kinetic energy (Alatorre-Ibargüengoitia et al. 2012). Such parameterization is relatively unconstrained by specific characteristics of the eruptive processes, and as a result, it produces general explosion scenarios. Here, we note that only the maximum launching kinetic energy is considered as the parameter that defines the explosion scenarios because during a single event, all the generated VBP may not be ejected with the same kinetic energy (Alatorre-Ibargüengoitia et al. 2006, 2012).

We defined three scenarios based on the launching kinetic energy associated with VBP ejected in different explosive events of El Chichón Volcano (Table 2). First, we considered the maximum ejection kinetic energy calculated for the VBP observed in the field

corresponding to two different eruptions. The '1982 eruption scenario' was defined considering the kinetic energy associated with the VBP with an average diameter of 19 cm that were launched to a maximum distance of 4.1 km from the crater during the 1982 eruption. The '550 BP eruption scenario' was defined in terms of the initial kinetic energy associated with 0.16-cm-diameter projectile found at 5.2 km from the crater ejected during the 550 BP eruption of El Chichón Volcano. Even when this is the ballistic projectile identified at the maximum distance in our field campaigns, we do not exclude the possibility of an eruption capable of ejecting VBP to yet larger distances. To account for this possibility, we then used an initial kinetic energy one order of magnitude higher than that associated with the '1982 eruption scenario' to estimate a 'yet-to-come scenario' that could affect a larger area.

The ballistic model presented in Sect. 3 was used so as to calculate the maximum kinetic energy of each of the VPB observed in the field, considering that the drag reduction close to the vent can be estimated from Eqs. (2) and (3) in accordance with the approach proposed by Fagents and Wilson (1993). The values of R_o and τ are not known, and in the case of El Chichón Volcano, they cannot be determined from field or video observations. From a number of simulations, we noticed that the value of τ is practically irrelevant as long as $\tau > 600$ (corresponding to $P_g/P_a = 100$ and $t_o = 6$ s), which is a reasonable assumption for all the explosion scenarios.

In this study, we consider $R_o = 500$ m to calculate the hazard zone associated with the '1982 eruption scenario' similar to the value considered by Fitzgerald et al. (2014) and in line with those found from numerical modeling of clasts coupled with a carrier flow field by de' Michieli Vitturi et al. (2010), $R_o = 700$ m for the zone associated with the '550 BP eruption scenario' and $R_o = 900$ m for the zone associated with the 'yet-to-come scenario.' The selection of the value of R_o does affect the calculations of the initial kinetic energy, and therefore, the obtained values have to be taken with caution. However, the uncertainties associated with the determination of parameters such as R_o and τ are minimized in the maximum range calculations if the same values are used consistently (as we did here) to compute the kinetic energy from the field measurements and subsequently to calculate the maximum distance that can be reached under optimum ejection conditions for the same kinetic energy (see below).

## 5 Volcanic ballistic projectile hazards map construction for El Chichón Volcano

The maximum range of the VBP for each explosion scenario is calculated considering the optimum launching conditions in terms of projectile diameter, launch angle, and wind velocity (Alatorre-Ibargüengoitia et al. 2012). The distance reached by the VBP as a

Table 2 Kinetic energies and optimum diameter associated with ballistic projectiles and corresponding maximum ranges and altitudes for the three explosion scenarios defined for el Chichón Volcano

Eruption scenario	Kinetic energy (J)	Maximum range (km)	Diameter with maximum range (m)	Total population	Maximum altitude (km asl)
1982 eruption	8.0×10^5	4.8	0.15	212	5.0
550 BP eruption	2.1×10^6	6.1	0.17	57	6.3
Yet-to-come	8.0×10^6	8.4	0.20	3441	8.0

The number of inhabitants in each zone (excluding the people living within the regions associated with the other scenarios) is also indicated (INEGI 2010)

Fig. 3 Ballistic range as a function of ballistic diameter for the three launching kinetic energies (*E*) corresponding to the explosion scenarios defined for El Chichón Volcano (without wind). *Dotted lines* indicate particle sizes whose movement is dominated mainly by the carrier flow and cannot be adequately described by a ballistic model
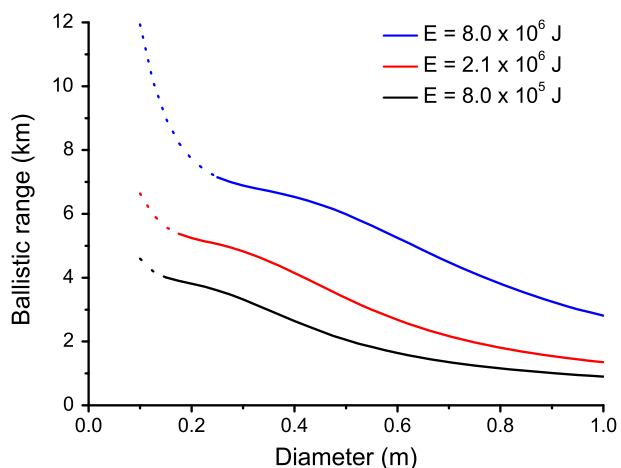
function of their diameter for each of the three different ejection kinetic energies corresponding to the defined explosion scenarios is presented in Fig. 3. It shows that the distance reached by the particles increases sharply if the diameter decreases below 15–20 cm (depending on the kinetic energy) since their trajectory is controlled mainly by the carrier flow and cannot be properly represented by a pure ballistic model. For this reason, the ballistic model was only applied to fragments which have average diameters larger than 15 cm. We also note that, for the same kinetic energy (E_k), the range reached by bigger fragments decreases with projectile size because the initial velocity v_o of larger particles is smaller $\left(v_o = \sqrt{\frac{2E_k}{m}} = \sqrt{\frac{12E_k}{\pi\rho_b D^3}}\right)$. In fact, we observed in the field that the VBP that were observed at maximum distances from the vent have average diameters around the ballistic limit, in accordance with the numerical calculations.

For a given size and initial kinetic energy, there is an optimum launch angle that allows VBP to reach the maximum distance. The altitude difference between the ejection and the landing points, the kinetic energy, and the projectile diameter are the factors that determine this optimal angle (Alatorre-Ibargüengoitia et al. 2006, 2012). After performing the calculations for every trajectory, we obtained that the optimum angles have values between 10° and 20° with respect to the horizontal axis. Additionally, a positive tailwind velocity can significantly increase the maximum range. For instance, we observe that a tailwind with the same direction of the projectile of 20 m/s ($\sim$70 km/hr) expands the maximum distance up to 15 %. Finally, it is worth noting that the VBP range depends also on the altitude because the drag force is proportional to air density, which decreases as a quadratic function of altitude (e.g., Waitt et al. 1995). For this reason, the VBP expelled by El Chichón Volcano will reach smaller distances than projectiles ejected by volcanoes with higher altitude.

The maximum distance that might be affected by the VBP according to our calculations considering the three explosion scenarios defined in Sect. 4 can be presented graphically in a hazard map as shown in Fig. 4. This map was created using altimetric digital models from the Instituto Nacional de Estadística, Geografía e Informática (INEGI) from 2000 processed with ArcGis®. Maximum ranges were computed considering optimum ejection conditions (diameter and angle) calculated for each scenario. Taking into consideration that our objective is to estimate the maximum possible ranges reached by the VBP, a
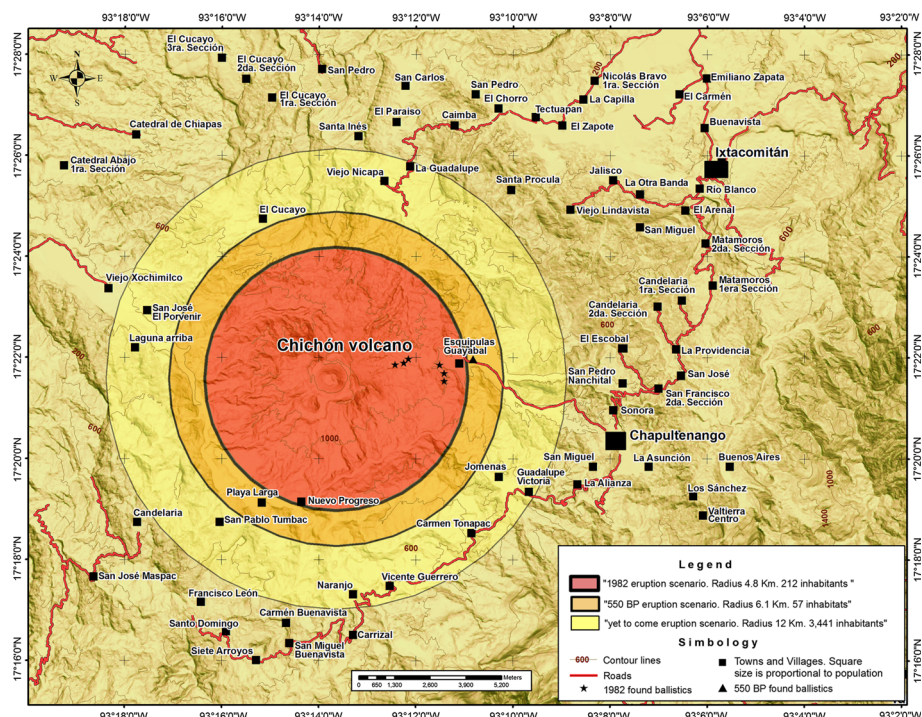
Fig. 4 Volcanic ballistic projectile hazard map for El Chichón Volcano. The map was prepared using altimetric digital models from the Instituto Nacional de Estadística, Geografía e Informática (INEGI), from the year 2000 with a resolution of 20 m with 20-m contour interval. Nowadays, there are people living again in villages such as Esquipulas Guayabal that were completely destroyed by the 1982 eruption. The number of inhabitants in each zone (excluding the people living within the regions associated with the other scenarios) is also indicated (INEGI 2010)

positive tailwind of 20 m/s was used in all the calculations regardless of the direction of the ejection as a reasonable higher limit. We observed that the altitude of the impact spots of the VBP does not change significantly in different ejection directions and therefore does not affect the expected range. For this reason, the hazard zones are circles with the diameter equal to the maximum range calculated for each scenario.

In addition to airborne ash that can seriously affect aerial navigation (e.g., Bonasia et al. 2012), VBP are considered to be also a great risk for aircraft in the surroundings of the volcano. This is especially important for scientists, civil protection authorities, and journalists, who frequently attempt to fly in the vicinity of the crater during volcanic crises for observing the crater conditions, monitoring purposes, or/and taking photographs (Alatorre-Ibargüengoitia et al. 2012). For this reason, it is also relevant to define vertical hazard zones. This is done by calculating the trajectories of VBP ejected with different angles and sizes and considering the highest altitude corresponding to each horizontal distance. This has to be done repeatedly for different distances from the crater up to the maximum distance that can be reached by the VBP (Alatorre-Ibargüengoitia et al. 2006, 2012). Even when throughout the simulations, the ejection velocity was not varied as a function of ejection angle, the model indicates that the VBP ejected at angles close to 90° move within the reduced drag zone for longer time and hence can reach relatively higher altitudes in

Fig. 5 Aerial hazard zones for ballistic projectile impact for El Chichón Volcano shown with the vertical profile north–south. The color code conventions corresponding to the three explosion scenarios are the same as in the hazard map (Fig. 4). North (N) and south (S) are indicated with the *arrow*
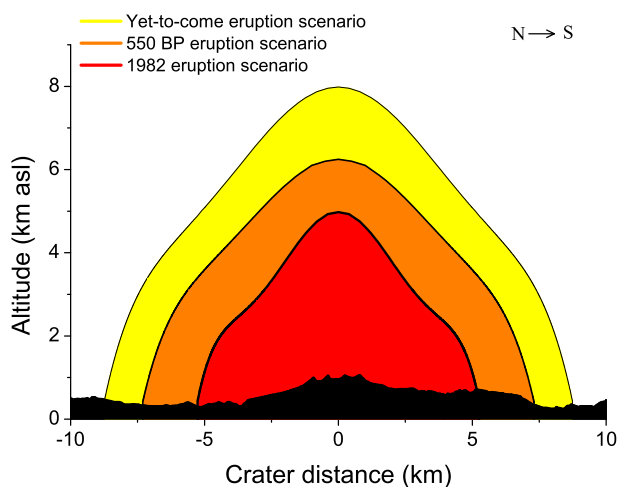
relation to VBP following more horizontal trajectories. The vertical hazard zones and maximum altitudes where impacts VBP are to be expected according to our calculations for the three explosion scenarios of El Chichón Volcano are presented in Fig. 5 and Table 2, respectively. The areas that have been outlined directly above the crater should be considered only as first-order estimations because the maximum altitude of the VBP in this region is expected to be controlled by the eruption dynamics which is not adequately described in our model.

The three-dimensional hazard zonation for each eruption scenario was represented through the various hazard zones on the VBP hazard map, along with the vertical profile. This graphical representation may support the responsible authorities to determine the horizontal and vertical restriction zones and to define prevention and mitigation actions in the case of a volcanic crisis.

6 Summary

Explosive volcanic eruptions frequently eject ballistic projectiles that are a significant threat to people's lives, infrastructure, and air navigation. We determine the hazards zones that can be likely be affected by VBP in three eruption scenarios defined for El Chichón Volcano considering its geological and historical past eruptive activity. Such scenarios were parameterized by calculating the maximum kinetic energy of the VBP observed in the field that were ejected during previous eruptions. The zone associated with the '1982 eruption scenario' was defined in terms of the maximum kinetic energy associated with the VBP produced in the 1982 eruption, whereas the second hazard zone associated with the '550 BP eruption scenario' was parameterized in terms of the kinetic energy associated with the VBP ejected in the 550 BP eruption. Finally, the zone associated with the 'yet-to-come scenario,' which is considered to be capable of ejecting the VBP to the farthest distance, was parameterized considering a kinetic energy one order of magnitude higher than the '1982 eruption scenario.' Assuming optimum launching conditions in terms of projectile diameter, launch angle, and positive tailwind velocity, we calculate the maximum range of the three scenarios to be 4.8, 6.1, and 8.4 km from the crater for the zones

associated with the '1982 eruption scenario,' the '550 BP eruption scenario,' and the 'yet-to-come scenario,' respectively. The calculations made for each of these scenarios allowed us to delimit the horizontal and vertical zones that can be affected by VBP. These zones are presented graphically on a VBP hazard map which shows the populated areas that can be affected by VBP impacts and a vertical profile indicating the hazard zones for aircraft in the vicinity of the volcano. The number of people threatened by VBP is 212, 57, and 3441 for each of the three scenarios (excluding the regions associated with other scenarios). Should the responsible authorities require to make development and mitigation plans and to define horizontal and vertical restricted areas throughout a volcanic crisis, they can use these graphical representations. The hazard map for ballistic impacts at El Chichón Volcano complements the hazard map published by Macías et al. (2008) which considers other volcanic hazards but not VBP.

References

Alatorre-Ibargüengoitia MA, Delgado-Granados H (2006) Experimental determination of drag coefficient for volcanic materials: calibration and application of a model to Popocatépetl volcano (Mexico) ballistic projectiles. Geophys Res Lett 33:L11302. doi:10.1029/2006GL026195

Alatorre-Ibargüengoitia MA, Delgado-Granados H, Farraz-Montes IA (2006) Hazard zoning for ballistic impact during volcanic explosions at Volcán de Fuego de Colima (Mexico). Geol Soc Am Spec Paper 402:26–39

Alatorre-Ibargüengoitia MA, Delgado-Granados H, Dingwell DB (2012) Hazards map for volcanic ballistic impacts at popocatépetl volcano (Mexico). Bull Volcanol 74:2155–2169. doi:10.1007/s00445-012-0657-2

Armienta MA, De la Cruz-Reyna S, Macías JL (2000) Chemical characteristics of the crater lakes of Popocatepetl, El Chichón, and Nevado de Toluca volcanoes, Mexico. J Volcanol Geotherm Res 97(1):105–125

Armienta MA, De la Cruz-Reyna S, Ramos S, Ceniceros N, Cruz O, Aguayo A, Arcega-Cabrera F (2014) Hydrogeochemical surveillance at El Chichón volcano crater lake, Chiapas, Mexico. J Volcanol Geotherm Res 285:118–128

Bonasia R, Costa A, Folch A, Macedonio G, Capra L (2012) Numerical simulation of tephra transport and deposition of the 1982 El Chichón eruption and implications for hazard assessment. J Volcanol Geotherm Res 231–232:39–49

Bower SM, Woods AW (1996) On the dispersal of clasts from volcanic craters during small explosive eruptions. J Volcanol Geotherm Res 73:19–32

Capaccioni B, Tarán Y, Tassi F, Vaselli O, Mangani F, Macías JL (2004) Source conditions and degradation processes of light hydrocarbons in volcanic gases: an example from El Chichón volcano, Chiapas State of Mexico. Chem Geol 206:81–96

Carey S, Sigurdsson H (1986) The 1982 eruption of El Chichón volcano, Mexico (2): observation and numerical modelling of tephra-fall distribution. Bull Volcanol 48:127–141

De la Cruz-Reyna S, Martin Del Pozzo AL (2009) The 1982 eruption of El Chichón volcano, Mexico: eyewitness of the disaster. Geofis Int 48(1):21–31

de' Michieli Vitturi M, Neri A, Esposti Ongaro T, Lo Savio S, Boschi S (2010) Lagrangian modeling of large volcanic particles: applications to vulcanian explosions. J Geophys Res 115:B08206. doi:10.1029/2009JB007111

Duffield WA, Tilling RI, Canul R (1984) Geology of Chichón volcano, Chiapas, Mexico. J Volcanol Geotherm Res 20:117–132

Espíndola JM, Macías JL, Tilling RI, Sheridan MF (2000) Volcanic history of El Chichón Volcano (Chiapas, Mexico) during the Holocene, and its impact on human activity. Bull Volcanol 62:90–104

Fagents SA, Wilson L (1993) Explosive volcanic eruptions-VII. The ranges of pyroclasts ejected in transient volcanic explosions. Geophys J Int 113:359–370

Fitzgerald RH, Tsunematsu K, Kennedy BM, Breard ECP, Lube G, Wilson TM, Jolly AD, Pawson J, Rosenberg MD, Cronin SJ (2014) The application of a calibrated 3D ballistic trajectory model to ballistic hazard assessments at Upper Te Maari, Tongariro. J Volcanol Geotherm Res 286:248–262

Instituto Nacional de Estadística Geografía e Informática (INEGI) (2010) Censo de población y vivenda 2010. INEGI, Mexico. http://www.inegi.org.mx

Konstantinou KI (2015) Maximum horizontal range of volcanic ballistic projectiles ejected during explosive eruptions at Santorini caldera. J Volcanol Geotherm Res 301:107–115

Layer PW, García-Palomo A, Jones D, Macías JL, Arce JL, Mora JC (2009) El Chichón volcanic complex, Chiapas, México: stages of evolution based on field mapping and 40Ar/39Ar geochronology. Geofis Int 48:33–54

Macías JL, Sheridan MF, Espíndola JM (1997) Reappraisal of the 1982 eruptions of El Chichón volcano, Chiapas, Mexico: new data from the proximal deposits. Bull Volcanol 59(6):459–471

Macías JL, Arce JL, Mora JC, Espíndola JM, Saucedo R, Manetti P (2003) The ∼550 BP Plinian eruption of el Chichón volcano, Chiapas, Mexico: explosive volcanism linked to reheating of a magma chamber. J Geophys Res 108(B12):2569. doi:10.1029/2003JB002551

Macías JL, Capra L, Arce JL, Espíndola JM, García-Palomo A, Sheridan MF (2008) Hazard map of El Chichón volcano, Chiapas, México: constraints posed by eruptive history and computer simulations. J Volcanol Geotherm Res 175:444–458

Mastin LG (2001) A simple calculator of ballistic trajectories for blocks ejected during volcanic eruptions. Open-file Report 01-45, US Geological Survey, Vancouver

Mora JC, Layer PW, Jaimes-Viera MC (2012) New 40Ar/39Ar ages from the Central Part of the Chiapanecan volcanic arc, Chiapas, México. Geofís Int 51(1):39–49

Rose WI, Bornhorst TJ, Halsor SP, Capaul WA, Lumley S, De la Cruz-Reyna S, Mena M, Mota R (1984) Volcán El Chichón, Mexico: pre-1982 S-rich eruptive activity. J Volcanol Geotherm Res 23:147–167

Rouwet D, Taran Y, Varley N (2004) Dynamics and mass balance of El Chichón crater lake, Mexico. Geofís Int 43:427–434

Scolamacchia T, Capra L (2015) El Chichón Volcano: Eruptive History. In: Scolamacchia T, Macias JL (eds) Active volcanoes of Chiapas (Mexico): El Chichón and Tacaná. Springer, Berlin, pp. 45–76

Swanson D, Zolkos S, Haravitch B (2010) Ballistic blocks surrounding Kilauea's caldera. Eos Am Geophys Union Trans 91:V33B–V0646B

Taddeucci J, Alatorre-Ibarguengoitia M, Palladino DM, Scarlato P, Camaldo C (2015) High-speed imaging of Strombolian eruptions: gas-pyroclast dynamics in initial volcanic jets. Geophys Res Lett 42:6253–6260. doi:10.1002/2015GL064874

Taran Y, Fisher TP, Pokrovsky B, Sano Y, Armienta MA, Macías JL (1998) Geochemistry of the volcano-hydrothermal sytem of El Chichón volcano, Chiapas, Mexico. Bull Volcanol 59:436–449

Tassi F, Vaselli O, Capaccioni B, Macías JL, Nencetti A, Montegrossi G, Magro G, Buccianti A (2003) Chemical composition of fumarolic gases and spring discharges from El Chichón volcano, Mexico: causes and implications of the changes detected over the period 1998–2000. J Volcanol Geotherm Res 13(1–2):105–121

Tilling RI, Rubin M, Sigurdsson H, Carey S, Duffield WA (1984) Prehistoric eruptive activity of El Chichón volcano, Mexico. Science 224:747–749

Tsunematsu K, Chopard B, Falcone J, Bonadonna C (2014) A numerical model of ballistic transport with collisions in a volcanic setting. Comput Geosci 63:62–69

Vanderkluysen L, Harris AJL, Kelfoun K, Bonadonna C, Ripepe M (2012) Bombs behaving badly: unexpected trajectories and cooling of volcanic projectiles. Bull Volcanol 74:1849–1858. doi:10.1007/s00445-012-0635-8

Waitt RB, Mastin LG, Miller TP (1995) Ballistic showers during crater peak eruptions of Mount Spurr volcano, summer 1992. USGS Bull 2139:89–106

Wilson L (1972) Explosive volcanic eruptions II. The atmospheric trajectories of pyroclasts. Geophys J R Astron Soc 30:381–392